

Evaluation of a Piezo-ceramic Sensor

Juan M. Lorenzo¹

Louisiana State University, Baton Rouge, Louisiana, 70803, U.S.A.

Donald A. Patterson²

Ario Labs LLC, Baton Rouge, Louisiana, 7081, U.S.A.

Renee Weber³

NASA Marshall Space Flight Center, Huntsville, 35805, U.S.A.

I. Abstract

Piezo-technology is widely used in the defense, aerospace and structural engineering fields. Current, off-the-shelf piezo-ceramic-type sensors can be used to develop miniature seismological instruments that permit non-invasive, shallow (< 1 m) high-resolution (10 cm) characterization of the regolith/soil profile on planetary bodies. We compare the signal-to-noise performance of a piezo-ceramic-type accelerometer to a proven, piezo-polymer-type sensor.

II. Introduction

A. Significance

Water is key for supporting future human missions on the Moon as well as Mars, and because buried H₂O ice can stiffen near-surface materials on these inner planetary bodies, seismic estimates of their strength have the potential to characterize the volume and distribution of buried H₂O ice. Specifically, high-frequency (kHz) seismic, piezo-electric sounding systems have the potential to reduce the ambiguity of in-situ resource mapping of the upper few m of regolith and soils and can complement other non-invasive methods which may not be able to penetrate as deeply (e. g., gamma, neutron, & radar spectroscopy). For this purpose, we envisage small arrays of piezo-sensors and piezo-sources integrated structurally into the landing pads of static landers (Figure 1) or rover wheels (Figure 2). A low-power and low-footprint seismic sub-system may characterize key aspects of the H₂O(s)-ice reservoirs foremost via their seismic velocities, and seismic attenuation calibrated to geomechanical and geotechnical properties.

Buried H₂O-ice reservoir characteristics such as depth, lateral continuity, distribution and degree of purity may enhance our understanding of volatile transport processes and growth within the lunar regolith and crust. Regolith in permanently shadowed regions of the Moon is key to understanding the genesis of the sequestered ice portion of the Lunar 'water' cycle¹ and to improving its potential as a sustainable resource for use by humans. Our focus lies within first few meters of the surface where potential ice-mining will be most feasible. In-situ characterization of H₂O-ice using landers or rovers, prior to excavation, helps preserve the geologic record of volatile deposition, and map sites suitable for mining.

¹ Professor, Department of Geology and Geophysics, Louisiana State University.

² Ario Labs LLC, 4055 Overlook Point Ct. Baton Rouge, LA 70817-1620, U.S.A.

³ Chief Scientist, NSSTC 2047, 320 Sparkman Dr., Huntsville, AL 35805, U.S.A

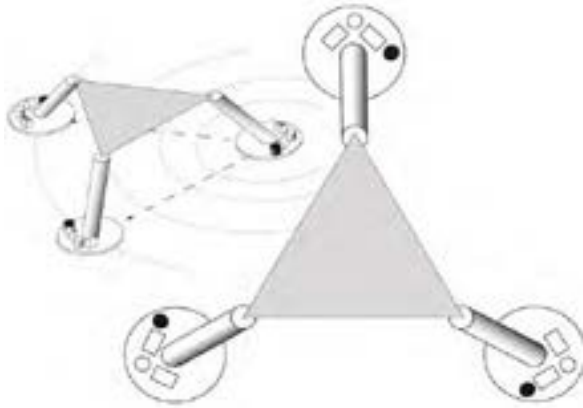


Figure 1. LEFT: Perspective view of conceptual lunar lander with payload area (triangle). Estimated ~ 2 m between landing pads. Piezo-actuators (black) create seismic pulses that travel between pads and sample the upper few meters of the lunar regolith. **RIGHT:** Three equally distributed piezo-sensors and one vertical piezo-actuator (green) are installed on each of 3 pads.

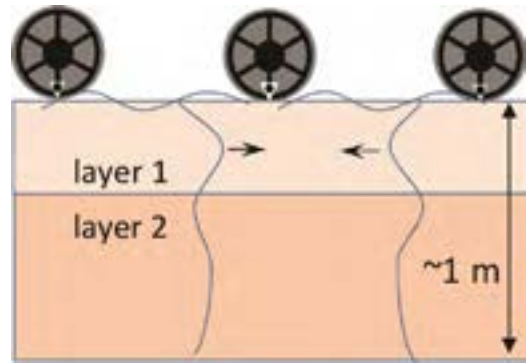


Figure 2. In concept, sensors (white triangles) and actuators (black circles) integrated into rover wheels can both generate and measure surface waves (blue curves). Multiple devices can be incorporated into each wheel. Seismic data are collected when the rover is stopped. Several seconds is sufficient to record data. Calibration against laboratory standards² may constrain estimates of ice-soil concentration.

Small piezo-electric sensors (1 cm x 1 cm footprint) can be used to extract soil properties under controlled laboratory conditions. However, redesign of these systems is needed for deployment under a much wider and more extreme range of physical conditions (e.g., temperature, radiation, accelerations). In a step toward space readiness, herein we evaluate and compare the performance of more suitable types of ceramic piezo-sensors against a standard high-performance polymer-based sensor.

B. Background to piezoelectric sensors and seismic instrumentation

Piezoelectric materials will produce an electric charge when stressed and conversely will change shape when subjected to an electric field. Piezoelectric materials have been widely used over the past 100 years, e.g., in radios and sonar. They have seen regular use since World War II in measuring and detecting shock waves from explosions (including atomic detonations) in environments up to 700°C (e.g.,^{3,4,5}).

In general, polymer-based piezoelectric transducers (polyvinylidene fluoride-PVDF) are about an order of magnitude more sensitive than piezo-ceramic and natural crystals, but they lose sensitivity and are expected to become brittle as they transition to a glassy-brittle state (< -35 °C), under space-temperature conditions. However, because they have been in use for decades in geotechnical soil studies^{6,7} they do provide convenient and low-cost laboratory analogs (Figure 3).

Nevertheless, compared to PZT sensors, PVDF types have a limited operational temperature range⁸. Typically, they operate from -40°C to 85°C. Above 120°C the polymer starts to approach its Curie temperature and melts around 170°C. Below 0°C the d_{31} parameters drop off sharply. In liquid Nitrogen (77°K), PVDF loses more than 99% of its sensitivity compared to PZT type sensors. At 77°K, the PZT also loses about 58% of its sensitivity but overall is still approximately 600 times more sensitive than the PVDF film. In addition, PZT and other types of ceramic sensors have Curie temperatures in excess of 200°C. Newer ceramic materials have even higher Curie temperatures, and for these reasons, ceramic type accelerometers are more appropriate for external mounting on a lunar lander.

Moreover, synthetic, piezo-transducers made of ceramic lead zirconate titanate materials (PZT, e.g., Figure 3) have long been under consideration by NASA⁹. Piezoelectric ceramics such as those that comprised the penetrometer (PZT-5A) on the Huygens lander were used to determine grain size of the surface of Titan. This material was chosen because of its sensitivity and durability to space temperatures and prolonged exposure to radiation levels over its 7-year mission. As well, for piezo-actuators which act as seismic source generators, lead magnesium niobate (PMN) and

PMN-PT (titanate) are examples of well-known electrostrictive materials (e. g., ¹⁰) currently available commercially (e. g., TRS technologies) for use especially in cryogenic (NIST-below 180° C) conditions¹¹.

Previous successful use of piezo-ceramics in space on the Cassini-Huygens probe on Titan¹² their current technological maturity, low cost, low power consumption (μA), low mass (Table 1: e.g., 4.5 g) make them novel candidates for a technological leap that was not available during the Apollo era. Although piezo-sensors have 3-4 orders of magnitude less sensitivity when compared to the nearest equivalent MEMS sensor technology of the shortest-period seismometers (SEIS-P¹³ : 0.5 ng/ $\sqrt{\text{Hz}}$ @ 10Hz) of the InSight mission to Mars, SEIS-P has lower bandwidth (~ 40 Hz) was not designed to image the soils of Mars but primarily, to remove environmental noise and aid the longer-period seismometer to detect mars-global seismic events. Piezo-sensors have several advantages because they have a broader bandwidth (kHz) and finer resolution than Apollo missions that allows them to detect properties of the shallow regolith structure (< 3 m) plus they can be coupled with nearby, conveniently small (1 cm^3) piezo-actuator seismic sources.

In order to determine the shallow structure (~ 300 m) of the lunar regolith, Apollo 14, 16 and 17 missions all employed active thumping (by astronauts) or explosions in their experiments¹⁴. But an envisaged static lunar lander will not have the ability to deploy an array of seismometers as did Apollo and a Huygen's-type probe will not be capable of determining geomechanical properties down to a few meters. Although outside the limit of this report, piezo-electric actuators can also fill that role with a small size (Figure 3).

C. Brief Outline

A PZT accelerometer is expected to be far more sensitive than a PVDF-polymer-based accelerometer under cold space conditions (liquid Nitrogen). Nevertheless, because these cold temperatures can reduce the PZT by about half, our goal herein is to evaluate whether we can increase the signal-to-noise ratio sensitivity of a PZT accelerometer, with reference to a PVDF polymer at room temperature, by introducing a newly designed differential charge amplifier. If so, then we expect that in a future stage, the same new electronics will also be tested at liquid Nitrogen conditions.

III. Tools and Methods

A. Background to Seismic Piezo-electric sensors

In previous upper soil seismic measurements^{2,7} the electronics are designed around the TE Connectivity ACH-01 PVDF type accelerometer with an integrated JFET (Figure 3E, Table 1). The PVDF-type sensor has a room temperature sensitivity of 10 mV/g and a low acoustic impedance for better coupling to loose soil types. The ACH-01 has three lines from the sensor: +12 VDC, GND, and a signal output from the sensor's internal low noise JFET. The sensor output is passed through a high pass filter with -3dB low frequency roll-off of 20 Hz. It is then passed through a low-noise instrument amplifier with two gain settings (x100 and x1000, Figure 3, Table 1). Since piezoelectric sensors all exhibit a pyroelectric effect, the instrument amplifier is auto-zeroed to eliminate low frequency drift due to temperature changes of the environment on the sensor. The amplified signal is input to a differential output amplifier to drive a twisted pair cable connected to the final differential input, data acquisition system.

Although the instrument described above works well in the terrestrial environment, we must increase the range of physical conditions under which these sensor systems must perform in space, such as on the landing pads of a lunar lander. Herein we address two changes in our system in order to extend the range of working temperatures toward cryogenic conditions, for example, as is expected in the permanently shadowed areas of the Moon. First, we use a new electronic design and incorporate a PZT-based commercial, off-the-shelf sensor (est. US\$ 400).

Commercially available PZT-type accelerometers usually contain an internal JFET to convert the charge generated into a voltage output. Most commonly, the other electrode of the sensor is connected to a metal casing and is grounded.

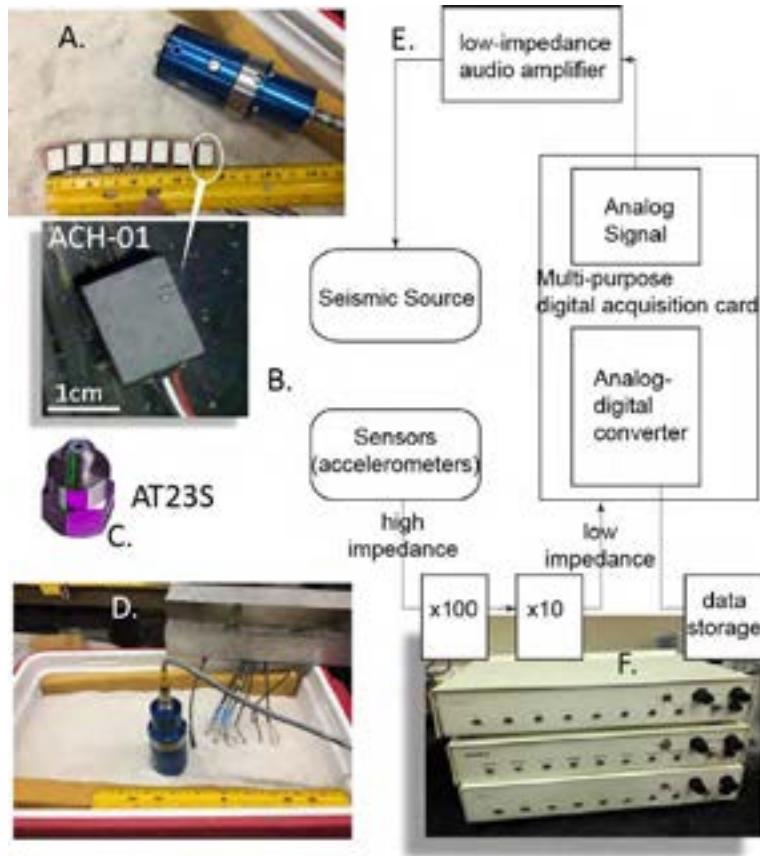


Figure 3. Sensor tests use (A) a magnetostrictive seismic source (blue cylinder) to compare polymer-based piezo-accelerometers (A & B) against a piezo-ceramic sensor (C) in a small sand tank (D) (E) Flow graph charts data acquisition steps¹⁵. Sensor voltage output is amplified x 100 (bottom right - F) and output as a differential-ended analog stream for digitization and data storage.

This type of circuit produces a single-ended output which is subject to external noise coupling. A better method is to take advantage of the differential nature of the piezoelectric element. Instead of producing a single-ended charge-to-voltage, two low-noise and matched JFETs can produce a floating differential current output. Since no commercially-available ceramic piezo-sensor comes with such a front-end circuit configuration, we choose a DJB Instruments A/23/TS (A23TS) charge-output sensor (Figures 3, 4), with no internal JFET, to prototype our customized differential JFET circuit, which is installed directly at its output. Gate bias resistors are selected to produce a -3dB low-frequency roll-off of 8 Hz. These two differential JFETs are biased with a 100 μ A current source and converted the sensor charge through a differential current output that is then sent through a twisted-pair cable to two, matched, transresistance amplifiers that convert the current to a voltage. These amplifiers are also filtered to produce an upper -3 dB frequency cutoff of 5 kHz. The differential voltage outputs of the transresistance amplifiers are then input to a gain-selectable, low-noise, differential instrument amplifier. Similar to the ACH-01 conditioning circuit (Figure 3, Table 1), the instrument amplifier contains an offset-zeroing circuit to compensate

for temperature effects and other component offsets. The amplified and filtered output also goes to a fully differential output amplifier that drives a twisted pair line connected to the same data acquisition input as for the ACH-01.

Seismic Sensors, Test and Acquisition System (Figure 3)

<i>Sensors</i>	
For ACH-01	Piezo-electric accelerometer of polyvinylidene fluoride film composition (ACH-01 from Tyco); onboard charge amplifier, nominally flat response of $\sim 9\text{mV/g} \pm 1\text{mV}$, in 20 Hz to 20 kHz frequency range, $\sim 8\text{ g}$.
AT23S	PZT, 4.5 g.
Signal conditioning	100 and 1000-fold operational amplifier with differential output (Figure 3).
Sensor array dimensions	8 sensors, 0.03-.87 m source-receiver offsets, $\sim 0.017\text{ m}$ sensor spacing.
<i>Digital Recording</i>	
Multi-purpose, digital acquisition card	(a) Onboard, PCI-based analog-to-digital acquisition (AD) card with an 8 differential-channel mode input (Model PCI-6251 from Nat. Instr.) software triggering, and low impedance analog output for source wavelet.
Instrument control software	Modified version of Multi-Function-Synch AI-AO.vi written in "G", a commercial virtual instrument software programming language (from National Instruments).
Sample rate	78.125 kS/s, per analog-input differential channel (8)
Nyquist frequency	$\sim 39\text{ kHz}$
Input and output resolution	1 in 16 bits; 305 mV in 16 bits; 305 mV range.
Acquisition format	LabView© (Natl. Instr) ASCII format converted to SEGY ¹⁶
Source wavelets	(a) Ricker wavelet, central frequency at 2 kHz, 23 samples at 50 kS/s, 50 micro-s wide side-lobes; synthesized digitally by PCI-6251 AD card. (b) Step-impulse, 20 kHz bandwidth
Seismic source generators	(a) Magnetostrictive ultrasonic transducer (Model CU- 18 from Etrema Products Inc.). Low-impedance audio amplifier (Model RMX 2450 from QSC Audio Products LLC) amplifies input Ricker source wavelet to drive this transducer at +150V (max)
Seismic software	Seismic Unix Processing System ¹⁷ , for filtering, manipulation and display.
	Oscilloscope-function generator with automatic Bode Plotter (Velleman PCSGU250)
	Mechanical shaker/vibrator (PASCO Scientific Model ST-9324)
	Digital function generator-amplifier (PASCO Scientific Model PI-9587A)

Table 1- Nominal field, source and sensor equipment and software, and seismic acquisition parameters for the laboratory experiments (adapted from ¹⁵)

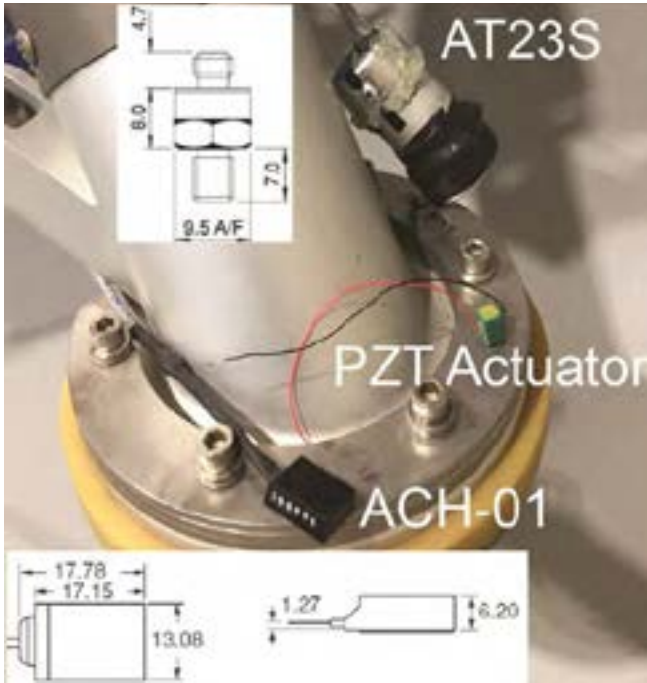


Figure 4. Mighty Eagle Lander pad and leg (NASA Marshall Space Flight Center) and two piezo-electric accelerometers (ACH-01 and AT23S) tested herein. The green piezo-stack actuator will be used in future development of a complete source plus sensor array. Both accelerometers are of comparable weight (Table 1) and size (all measurements are shown in mm). An aluminum cylinder is *only* a temporary, oversized housing to stabilize air moisture content for the front-end electronics.

B. Bode Plots

Generally, piezo-polymer sensors are an order of magnitude more sensitive than piezo-ceramic sensors. However, the major advantage of piezo-ceramics is their proven reliability and performance in space. Polymer-based sensors become brittle at low temperatures and show a marked reduction in their performance.

In order to compare the frequency and phase response characteristics of the ACH-01 against the AT23S, (Table 1) we use proprietary, automated, Velleman software (PCSGU250 V.114). We average all responses at each frequency for 2 s, over 0-10 kHz and normalize the output to the input Voltage (Figure 5). Low-frequency thresholds are different and conditioned by electronics.

Both the ACH-01 and AT23S display a similar phase shift response, in the most useful frequency ranges: $< 10^3$ Hz. The amplitude gain of the AT23S exceeds that of the ACH-01 and shows a linear increase with frequency (Figure 5). The equivalent response for the ACH-01 stays flat and nearly constant as per manufacturer's specification.

Overall, Bode plots show that the AT23S appears to be more sensitive. However, because the amplifiers for the ACH-01 and AT23S are not currently matched we prefer to conduct an additional signal-to-noise evaluation under common experimental conditions. We do expect the ACH-01 to be more sensitive at room temperatures, but we want to evaluate the relative benefit of our redesigned circuitry for the AT23S. Two, matched, onboard JFET charge amplifiers should improve the signal-to-noise which is a more useful indicator of usability of these tools in space conditions.

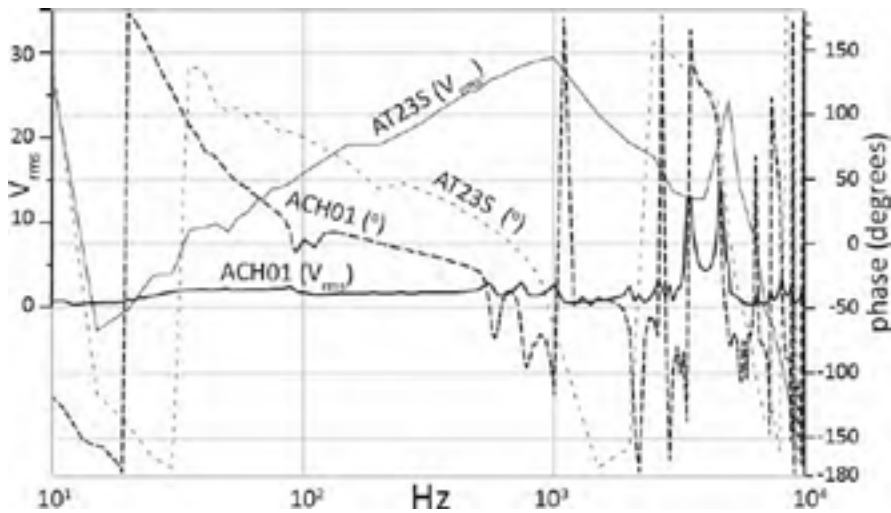


Figure 5. Gain (V_{rms}) and phase response of a polymer-based piezo-sensor (ACH-01, \$30) compared to a piezo-ceramic sensor (AT23S-\$400). Although typically less sensitive, the AT23S response is improved with onboard differential charge amplifiers and additional amplifiers prior to data acquisition. (Figure 2, Table 1). We note that pre-amplifiers with increase gain. For reference, off-the shelf cryogenic-rated sensors cost ~US \$1000.

C. Signal-to-Noise Evaluation



Figure 6. Spatial arrangement of sensor and source for AT23S sensor. Separation between repeated locations of the magnetostrictive shaker/vibrator = 5 cm. The first offset between the source and the nearest sensor is 3.8 cm. Grain diameter: $< 2^{-4}$ mm



Figure 7. Spatial arrangement of sensor and source for case of ACH-01 sensors. Fixed location of magnetostrictive shaker/vibrator, but ACH-01 sensors are buried 1 cm, and separated 5 cm apart. The first offset between the source and the nearest sensor is 3.8 cm. Grain diameter: $< 2^{-4}$ mm.

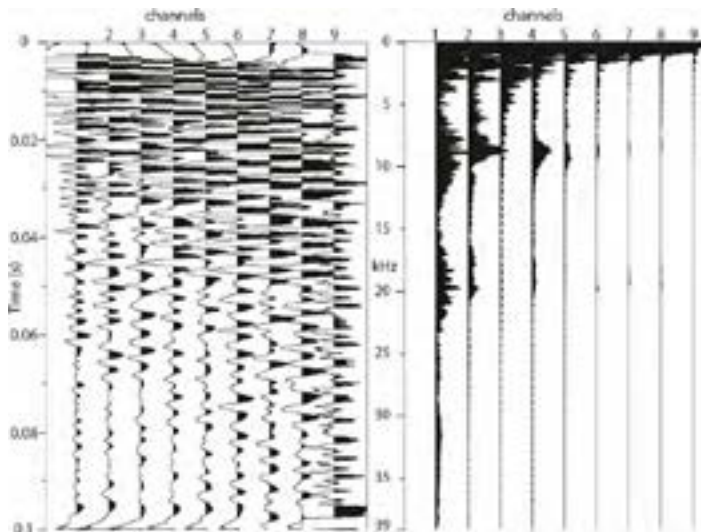


Figure 8. Representative data collected for the AS23S sensor. (LEFT) Channels 1 through 8 indicate variations of recorded voltage output versus time and offset (5 to 40 cm) between the sensor and a moving magnetostrictive shaker/vibrator-- and channel 9 contains background noise. (RIGHT) Equivalent amplitude spectra for each respective channel, including that containing background noise (channel 9).

We derive a useful comparison of signal-noise-ratio (SNR) between sensors for a common experimental setup in a sand box containing very fine-to-silt sized, angular quartz sand (Figures 6 and 7). We analyze the change in energy among the different frequency components of the data (Figure 8) as a function of fixed distances (offsets) between a mechanical vibrator/shaker and sensors. We do not consider the energy contribution from the phase component. In order to estimate the signal-to-noise (in the frequency domain – Figure 9) we total the ratios of the data energy at each frequency to that found in the common background noise which is collected when the shaker is turned off. The original seismic vibration that enters the sand at the shaker/vibrator is designed to be a Ricker wavelet with a dominant

frequency of 2 kHz. But, by seismic attenuation through the sand, dominant frequency is reduced to < 1 kHz when it is received at the sensors.

Thanks to careful mechanical sieving, we can assume that sand body is sufficiently homogeneous so that only the distance between the sensor and the shaker will affect signal quality. That is, the nature of the seismic signal is dominated only by relative distance between the source and the sensor because the medium properties are laterally constant. As in the case of our single AT23S sensor, we record both seismic data and background noise while the sensor remains fixed at one end of the sand box, but the source-to-sensor offset varies from 5-to-40 cm (Figure 6). For each recording, the shaker is placed at eight different locations across the sand box 5 cm apart (Figure 6). In the case of the ACH-01, 8 sensors placed in a line and separated by 5 cm (Figure 7) also record seismic data for the full range of sensor-to-shaker offset, as well as the background noise but with the shaker fixed at one end of the sand box. Experiments for both sensor types share a common wavefield and any possible edge effects are similarly shared, so that in practice we are able compare the SNR under identical conditions².

IV. Results and Recommendations

Newly designed electronics for a PZT-type sensor (AT23S) show that, although a PVDF-type sensor (ACH-01) displays a better signal-to-noise ratio (SNR) at room temperature, the PZT-type sensor can achieve a similar-order SNR as the ACH-01 (Figures 9 and 10). Specifically, SNR tests of the ACH-01 and its amplifier show a maximum value of ~ 160 centered at ~ 800 – 900 Hz, whereas the SNR of the AT23S is ~ 140 at ~700 Hz. Future experiments will focus on improvement of new electronics (1) to flatten a linear spectral response (Figure 5) that is observed for the AT23S and (2) to temperature-harden the electronic components so that we can continue (3) to test PZT sensor performance as well as piezo-ceramic type shakers/vibrators under liquid nitrogen temperatures.

In future work, causes in the secondary differences of the SNR between sensor types attributable to variable experimental conditions should be addressed as well. Variations can arise from differences in the mechanical coupling between different sensor enclosures (plastic versus Aluminum) to the sand body, enclosure resonance, cabling distribution, edge effects and the presence of various tools in the sand tank during the experiments (cf. Figures 6 and

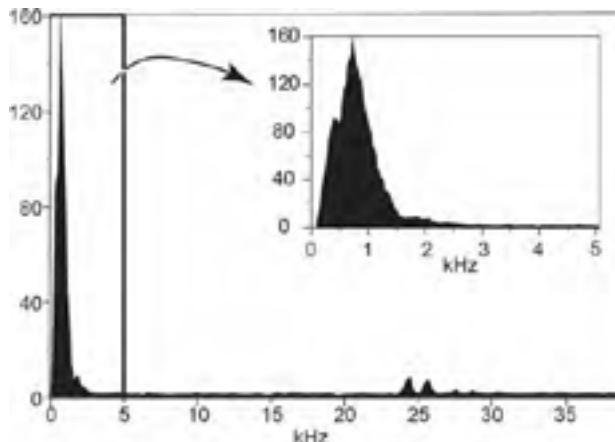


Figure 9. Signal-to-noise-variation ratio for a polymer-based ACH-01 sensor, up to the Nyquist frequency (~39 kHz), in a laboratory experiment. Usable frequencies reach ~5 kHz at most.

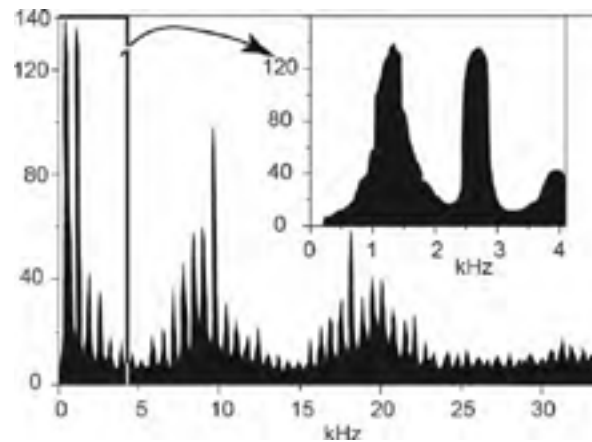


Figure 10. Signal-to-noise-variation ratio For a PZT-based AT23S sensor, up to the Nyquist frequency (~39 kHz) data in a laboratory experiment. Usable frequencies reach ~5 kHz.

7). Although similar experimental variations have not apparently influenced seismic analyses in past experiments² future investigations should remain vigilant. We envisage future use of miniature piezo-electric sensors and shakers/vibrators on landers and rovers to help interrogate for shallow (few meters) buried in-situ resources.

V. Acknowledgments

The first author thanks F. Dix of the Marshall Faculty Fellowship program for providing the opportunity to collaborate with members of the Lunar Planetary Science group at the National Space Science and Technology Center during my stay at the Marshall Space Flight Center, Huntsville, Alabama. Renee Weber was pivotal in providing space and a welcoming research environment together with H. Haviland-Fuqua, C. Fassett and M. Zanetti.

VI. References

- ¹Jawin, E. R., Valencia, S. N., Watkins, R. N., Crowell, J. M., Neal, C. R., and Schmidt, G., “Lunar Science for Landed Missions Workshop Findings Report: Earth and Space Science”, 2019, Vol. 6, No. 1, pp. 2-40.
- ²Lorenzo, J. M., Patterson, D. A., Karunatillake, S., Weber, R., Haviland, H., and Fassett, C., “Seismic Characteristics of the Shallow (0–1 m) Soils on the Moon and Mars: Ice in Soils”, *50th Lunar and Planetary Science Conference*, 2019, Houston, Lunar and Planetary Institute, Abstract #3246.
- ³Dietrich, R. V., *The Tourmaline Group*, New York, Van Nostrand Reinhold Company, 1985, pp.1-300.
- ⁴Tressler, J., Alkoy S, and Newham, R. E., “Piezoelectric sensors and sensor materials”: *J Electroceram*, 1998, Vol. 2, pp. 257-272.
- ⁵Zu, H., Wu, H., and Wang, Q.-M., “High-Temperature Piezoelectric Crystals for Acoustic Wave Sensor Applications”: *IEEE transactions on ultrasonics, ferroelectrics, and frequency control*, 2016, Vol. 63, No. 3, pp. 486-505.
- ⁶Santamarina, J., Wakim, T., Tallin, A., Rab, F., and Wong, J., “Piezo film technology and applications in geotechnical testing”, *Geotechnical Testing Journal*, 1991, Vol. 14, No. 4, pp. 363-370.
- ⁷Lorenzo, J.M., Hicks, J., Vera, E.E., “Integrated seismic and Cone Penetration Testing observations at a distressed earthen levee: Marrero, Louisiana, U.S.A.”, *Engineering Geology. Journal of Engineering Geology* 2014, Vol.168C, pp. 59-68.
- ⁸Martinez, C., Zheng, Y., Daniel Easton, D., Kevin Farinholt, K., and Gyuhae Park, G., “Strain Sensors for High Field pulse Magnets”, *27th Conference and Exposition on Structural Dynamic 2009: (IMAC XXVII)*; Orlando, Florida, USA,200 9-12 February 2009, Vol. 1
- ⁹Hooker, M. W., “Properties of PZT-Based Piezoelectric Ceramics Between -150 and 250 C”, 1998 NASA Langley Research Center; Hampton, VA United States.
- ¹⁰Blackwood, G. H., and Ealey, M. A., “Electrostrictive behavior in lead magnesium niobate (PMN) actuators. I. Materials perspective”, *Smart Materials and Structures*, 1993, Vol. 2, No. 2, pp. 124-133.
- ¹¹Xu, T.-B., Tolliver, L., Jiang, X., and Su, J., “A single crystal lead magnesium niobate-lead titanate multilayer-stacked cryogenic flextensional actuator”, *Applied Physics Letters*, 2013, Vol. 102, No. 4, p. 042906.
- ¹²Lorenz, R. D. (1994) *Measurement Science Technology* 5, 1003-1041.
- ¹³Bowles, N. E., Pike, W. T., Teanby, N., Robert, G., S. B. Calcutt, J. Hurley, P. Coel, J., Wookey, Dunton, P., Standley, I., Temple, J., Irsha, R., Taylor, J , Warre, T., and Charalambous, C., “Performance and Noise modelling of the Short Period Seismometer SEIS-SP, part of the SEIS instrument for NASA’s 2016 InSight Mission”, *LPSC 2015*, Houston.
- ¹⁴Cooper, M. R., Kovach, R. L., and Watkins, J. S., “Lunar near-surface structure”, *Reviews of Geophysics*, 1974, Vol. 12, No. 3, pp. 291-308.
- ¹⁵Lorenzo, J. M., Smolkin, D. E., White, C., Chollett, S. R., Sun, T. “Benchmark hydrogeophysical data from a physical seismic model”, *Computers & Geosciences* 2013 Vol. 50, pp. 44-5. Data sets downloadable from (<http://github.com/cageo/Lorenzo-2012>)
- ¹⁶Barry, K. M., Cavers, D. A., and Kneale, C. W., “Report on recommended standards for digital tape formats”, *Geophysics*, 1975 Vol. 40, No. 2, pp. 344-352.
- ¹⁷Stockwell, J.W., “The CWP/SU: Seismic Unix package”, *Computers & Geosciences*, 1999, Vol. 25, pp. 415-419.